MOLECULAR AND CELLULAR BIOLOGY, Oct. 2007, p. 7291–7301 Vol. 27, No. 20
0270-7306/07/$08.00+0 doi:10.1128/MCB.00773-07

Analysis of Endogenous LRP6 Function Reveals a Novel Feedback Mechanism by Which Wnt Negatively Regulates Its Receptor[▽]

Zahid Khan, Sapna Vijayakumar, Teresa Villanueva de la Torre, Sabrina Rotolo, and Anna Bafico*

Department of Oncological Sciences, Mount Sinai School of Medicine, New York, New York 10029

Received 2 May 2007/Returned for modification 25 May 2007/Accepted 26 July 2007

The canonical Wnt pathway plays a crucial role in embryonic development, and its deregulation is involved in human diseases. The LRP6 single-span transmembrane coreceptor is essential for transmission of canonical Wnt signaling. However, due to the lack of immunological reagents, our understanding of LRP6 structure and function has relied on studies involving its overexpression, and regulation of the endogenous receptor by the Wnt ligand has remained unexplored. Using a highly sensitive and specific antibody to LRP6, we demonstrate that the endogenous receptor is modified by N-glycosylation and is phosphorylated in response to Wnt stimulation in a sustained yet ligand-dependent manner. Moreover, following triggering by Wnt, endogenous LRP6 is internalized and recycled back to the cellular membrane within hours of the initial stimulus. Finally, we have identified a novel feedback mechanism by which Wnt, acting through β-catenin, negatively regulates LRP6 at the mRNA level. Together, these findings contribute significantly to our understanding of LRP6 function and uncover a new level of regulation of Wnt signaling. In light of the direct role that the Wnt pathway plays in human bone diseases and malignancies, our findings may support the development of novel therapeutic approaches that target Wnt signaling through LRP6.

The highly conserved canonical Wnt pathway plays a critical role in cell fate determination and tissue development (7, 23). Moreover, aberrant activation of Wnt signaling is causally involved in human cancers (9, 28). Members of this family of secreted glycoproteins interact with two coreceptors, the Frizzled seven-pass transmembrane receptor and the low-density lipoprotein (LDL) receptor-related protein LRP5/6. Wnt-receptor interactions lead to inhibition of β-catenin phosphorylation by casein kinase 1-α (CK1-α) and glycogen synthase kinase-β, which occurs within a protein complex containing axin and the tumor suppressor adenomatous polyposis coli. Inhibition of β-catenin phosphorylation impairs its degradation and results in accumulation of the uncomplexed cytosolic molecule, which translocates to the nucleus and interacts with TCF/LEF factors to activate transcription (9, 13, 24).

Frizzled receptors are known to mediate signaling through both the Wnt–β-catenin "canonical" pathway and other, "non-canonical" ones, such as the planar cell polarity and Wnt/Ca^{2+} pathways. In contrast, the LRP6 receptor and the family member LRP5 specifically function in the Wnt–β-catenin pathway (5, 13, 17). In fact, inactivation of the LRP5/6 homologue *arrow* in *Drosophila melanogaster* results in a phenotype similar to that of the *wingless* mutant, and injection of LRP6 mRNA into *Xenopus laevis* embryos enhances Wnt-induced developmental defects (33, 35). Moreover, mice deficient for LRP6 exhibit defects resembling those caused by the loss of various Wnt proteins (27). There is evidence supporting a dual-receptor model in which independent binding of Wnt to Frizzled and LRP6 recruits these two proteins into a receptor complex that triggers signaling (14). Although the mechanism involved in transmission of the Wnt signal to intracellular components is not fully understood, it is known that following Wnt binding, LRP5/6 is phosphorylated on a series of amino acid motifs present on its cytoplasmic domain (34). LRP5/6 phosphorylation leads to the recruitment of the scaffolding protein axin to the cell membrane (22). Recently, two studies identified glycogen synthase kinase-β and CK1 as the kinases responsible for LRP6 phosphorylation (11, 39).

LRP5/6 is a single-pass transmembrane protein containing a large extracellular domain composed of four YWTD propeller domains, with each followed by an epidermal growth factor domain and three LDLR domains. Truncation mutants lacking the extracellular domain are constitutively active, while deletion of the intracellular region results in a dominant-negative receptor (14). In addition to Wnt, LRP5/6 functions as the receptor for the Dickkopf (Dkk) family of secreted antagonists, which function as specific inhibitors of canonical Wnt signaling (3, 21, 32).

Ligand regulation of receptor trafficking between the cell surface and the endosomal compartment is an important aspect of receptor function (26, 37). It has been reported that Wnt5a induces the internalization of Fz4 through the binding of Dvl to β-arrestin 2 and that this internalization requires protein kinase C activation (8). Although recent evidence suggests that Wnt3a induces internalization of LRP6 (38), the mechanism by which the receptor is regulated by its ligand has not yet been investigated.

Our understanding of LRP6 structure and function has relied on studies involving its overexpression, while analysis of the receptor under physiologic conditions has been lacking. In the present study, using a new, highly sensitive anti-LRP6 monoclonal antibody (MAb), we demonstrate that endogenous LRP6 is posttranslationally modified by glycosylation, is present at the membrane in a dimeric form, and is phosphor-

* Corresponding author. Mailing address: Department of Oncological Sciences, The Mount Sinai School of Medicine, Box 1130, One Gustave L. Levy Place, New York, NY 10029. Phone: (212) 659-5543. Fax: (212) 987-2240. E-mail: anna.bafico@mssm.edu.

▽ Published ahead of print on 13 August 2007 .

ylated in response to Wnt in a sustained but ligand-dependent manner. Cell surface biotinylation analysis revealed that Wnt induces LRP6 internalization followed by its recycling to the cellular membrane. Importantly, our analysis uncovered a novel feedback regulation of LRP6 by which Wnt, through the downstream effector β-catenin, inhibits its receptor at the transcriptional level.

MATERIALS AND METHODS

Cell culture and gene transduction. NIH 3T3 cells were maintained in Dulbecco's modified Eagle's medium (DMEM) containing 10% calf serum. 293T cells and the human tumor cell lines MDAMB157 (breast), DU145 (prostate), HCT116 (colon), PA-1 (ovarian), and HeLa (cervical) were maintained in DMEM supplemented with 10% fetal bovine serum. The immortalized mammary epithelial cell line AB589 was cultured in the same medium in the presence of dexamethasone (Sigma) at 1 μM. Control and Wnt3a-conditioned media were collected from L cells and L cells/Wnt3a (ATCC) according to the manufacturer's instructions. Alternatively, recombinant purified Wnt3a (R&D Systems) was utilized at 100 ng/ml unless otherwise indicated. DKK1-conditioned medium was produced following transient transfection of 293T cells as previously described (3).

For viral infection, 5×10^5 NIH 3T3, NIH 3T3/Wnt3a, or AB589 cells in 60-mm plates were seeded in growth medium with 2 μg/ml Polybrene. Twenty-four hours later, cells were infected with viral supernatants produced as previously described (2). Cells were selected for 2 weeks with Geneticin (750 μg/ml), puromycin (2 μg/ml), or hygromycin (100 μg/ml). pCMV-LRP5-Flag and pCMV-LRP6-Flag cDNAs were transfected using Fugene (Roche) according to the manufacturer's instructions.

Western blot, immunoprecipitation, and glutathione *S*-transferase (GST)–E-cadherin binding assays. For Western blotting and immunoprecipitation assays, cells were solubilized in lysis buffer (10 mM sodium phosphate, 0.15 M NaCl, 1% NP-40, and a cocktail of phosphatase and protease inhibitors). For immunoprecipitation, cell lysates were incubated with a specific antibody (anti-axin 1, 5 μg/ml; and anti-LRP6, 5 μg/ml) and then with protein G beads (Pharmacia). After sodium dodecyl sulfate-polyacrylamide gel electrophoresis (SDS-PAGE) and transfer, membranes were blocked in 5% bovine serum albumin and incubated with the following primary antibodies at the indicated dilutions: anti-Flag, 1:1,000 (Sigma); anti-LRP5, 1:1,000 (Orbigen); anti-tubulin, 1:10,000 (Sigma); anti-actin, 1:30,000 (Sigma); anti-axin, 1:1,000 (Zymed); anti-N-cadherin, 1:500 (Sigma); antihemagglutinin (anti-HA) MAb, 1:1,000 (Hybridoma Center, Mount Sinai School of Medicine, NY); anti-phospho-LRP6 (Ser1490), 1:1,000 (Cell Signaling); anti-p53, 1:1,500 (Novo Castra); anti-platelet-derived growth factor receptor (anti-PDGFR), 1:2,000 (Santa Cruz); anti-TCF4, 1:1,000 (Upstate); and the MAb to LRP6, 1:1,000 (generated in collaboration with the Hybridoma Center, Mount Sinai School of Medicine, NY). Detection was performed by enhanced chemiluminescence (ECL) or, alternatively, with an Odyssey infrared imaging system (LI-COR). For phosphatase treatment, 293T cells were detached from the plates with phosphate-buffered saline (PBS)–EDTA (5 mM), divided into two aliquots, and lysed in either the presence or absence of phosphatase inhibitors. The latter aliquot was then subjected to λ-phosphatase (New England BioLabs) treatment for 1 h at 37°C and then incubated at 65°C for 1 h. Treated and untreated lysates were analyzed by Western blotting. A glycosidase reaction was carried out by incubating denatured cell lysates with peptide *N*-glycosidase F (PNGase F) (NEB) according to the manufacturer's instructions.

The GST–E-cadherin binding assay has been described previously (1). Bacterially expressed GST–E-cadherin was purified with glutathione-Sepharose beads (Amersham) and incubated with total cell lysates (0.5 to 1.0 mg). Following bead recovery and SDS-PAGE, uncomplexed β-catenin was detected with a MAb to β-catenin (BD Biosciences).

Membrane biotinylation and chemical cross-linking. Cells washed with PBS (Invitrogen) were incubated at 4°C, first with sulfo-NHS-LC-biotin (Pierce) for 30 min and then with 20 mM Tris-HCl (pH 7.5) for 20 min, to quench the reaction. After being washed in PBS, cells were solubilized in lysis buffer and incubated with immobilized avidin beads (Pierce) for 1 h. Beads washed three times in lysis buffer were subjected to SDS-PAGE and immunoblotting.

For cross-linking assays, cells washed twice with PBS to remove the culture medium were incubated with 2 mM thiol-cleavable DTSSP (3,3′-dithiobis[sulfosuccinimidylpropionate]) (Pierce) or noncleavable BS3 (Pierce) for 30 min at room temperature. The cross-linker was quenched with 20 mM Tris-HCl, pH 7.5, for 15 min. Cell lysates were immunoprecipitated with anti-LRP6 MAb and protein G-Sepharose (GE Healthcare). Immunoprecipitates and total lysates were resolved by SDS-PAGE and analyzed with the LRP6 MAb.

RNA interference. The previously described 19-nucleotide target sequence for LRP6 (2) was cloned into a lentiviral vector containing a puromycin-selectable marker (unpublished data). The lentiviral vector was cotransfected with envelope and packaging vectors in 293T cells, utilizing Fugene (Roche) according to the manufacturer's instructions. Lentivirus supernatant was collected at 48 and 72 h. For infection, 5×10^5 293T cells were infected and selected with puromycin (2 μg/ml) for 2 weeks.

Metabolic labeling. Cells were grown in phosphate-free DMEM (Invitrogen) supplemented with 10% dialyzed fetal bovine serum for 18 to 24 h. Phosphate-depleted cells were metabolically labeled with 0.35 mCi [^{32}P]orthophosphate (Amersham Biosciences) for 3 h. For experiments with recombinant purified Wnt3a, cells were preincubated with [^{32}P]orthophosphate for 1 h and further labeled for an additional 2 h in the presence of Wnt3a. Lysates were subjected to immunoprecipitation with the anti-LRP6 MAb, followed by SDS-PAGE, transfer to an Immobilon polyvinylidene difluoride membrane (Millipore), and autoradiography. The same membrane was probed with the LRP6 MAb and analyzed by ECL.

Real-time PCR. Total RNAs were extracted from cell lines by using TRIzol (Invitrogen) following the manufacturer's protocol. First-strand cDNA synthesized using random hexamers (Invitrogen) was used for real-time PCR (DNA Engine Opticon 2; Bio-Rad). Each PCR, done in triplicate, consisted of 10-fold-diluted first-strand cDNA as the template, FastStart SYBR green master mix (Roche Applied Science), and 500 nM of either LRP6 or TATA box binding protein primers. The PCR conditions used were 95°C for 15 min, followed by 40 cycles of 94°C for 10 seconds, 61°C for 20 seconds, and 72°C for 30 seconds. Melting curve analysis was conducted to ensure the specificity of the reactions, as recommended by the manufacturer's protocol (DNA Engine Opticon 2; Bio-Rad). The results were analyzed using Opticon2 software (Bio-Rad). The following primers were utilized: for mouse LRP6, 5′-AGGGTGGAATGAGTGT GCCT-3′ (forward) and 5′-TGATGGCGCTCTTCTGACTGA-3′ (reverse); and for mouse TATA box binding protein, 5′-ACATCTCAGCAACCCACACA-3′ (forward) and 5′-CAGCCAAGATTCACGGTAGA-3′ (reverse).

Northern blotting. Total RNA was isolated using TRIzol (Invitrogen) according to the manufacturer's instructions. Twenty micrograms of total RNA was subjected to electrophoresis (1% agarose in morpholinepropanesulfonic acid [MOPS]-formaldehyde). RNAs were transferred to a nylon membrane (Amersham Biosciences), and prehybridization was carried out for 2 h at 68°C in ExpressHyb hybridization solution (BD Biosciences). Hybridization was performed overnight under the same conditions, but with a radiolabeled probe. Membranes were washed twice in 2× SSC (1× SSC is 0.15 M NaCl plus 0.015 M sodium citrate)–0.05% SDS at room temperature and twice in 0.1× SSC–0.1% SDS at 50°C for 15 min. After being washed, the membranes were exposed to X-ray film at −80°C.

siRNA targeting of clathrin. Small interfering RNA (siRNA) oligonucleotides directed against human clathrin, as previously described (6), were custom ordered from Invitrogen (sense, 5′-GCAAUGAGCUGUUUGAAGATT-3′; and antisense, 5′-UCUUCAAACAGCUCAUUGCTT-3′). The oligonucleotides were resuspended in RNase-free water and annealed in a buffer containing 20 mM potassium acetate, 6 mM HEPES, pH 7.4, and 400 nM magnesium acetate. HeLa cells were transfected with the annealed oligonucleotides (10 nM), using siPORT NeoFX agent (Ambion) following the manufacturer's instructions. After 48 h, the efficiency of knockdown was monitored by Western blotting using an anti-clathrin antibody (BD Biosciences).

RESULTS

Characterization of a highly specific MAb against LRP6. The lack of sensitive antibodies to LRP6 has so far limited characterization of this receptor to studies involving its overexpression in model cells. Thus, we generated a series of MAbs against the LRP6 cytoplasmic domain. Expression vectors containing Flag-tagged human LRP6 and LRP5 cDNAs were transiently transfected into 293T cells, and the different antisera were tested by immunoblotting in comparison with a commercial anti-Flag antibody. Analysis with anti-Flag antibody re-

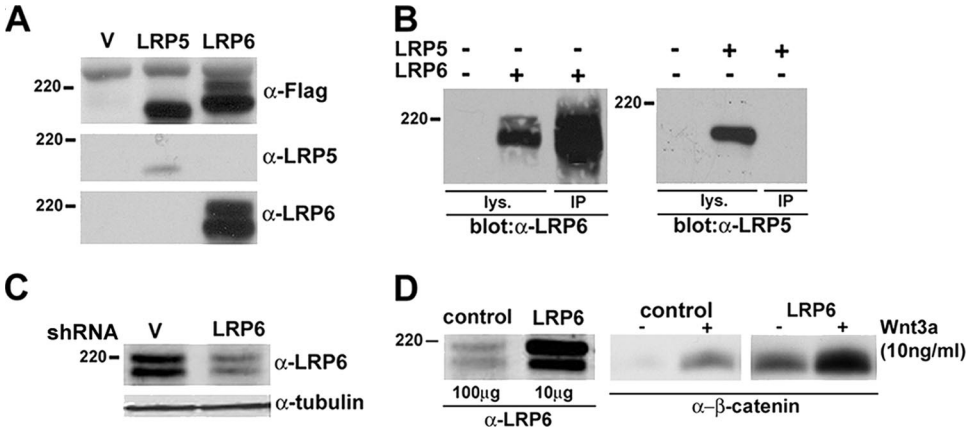

FIG. 1. Characterization of a MAb highly specific to LRP6. (A) Detection of human LRP5 and LRP6 following transfection into 293T cells. Cells were transfected with the indicated plasmids (1 μg), and at 48 h, cell lysates were subjected to immunoblot analysis with either anti-Flag (Sigma), anti-LRP5 antiserum (Orbigen), or the anti-LRP6 MAb (clone 1C10). (B) Immunoprecipitation of human LRP6 or LRP5 overexpressed in 293T cells. Forty-eight hours following transfection, lysates were subjected to SDS-PAGE directly (100 μg) or after immunoprecipitation (700 μg) with the anti-LRP6 MAb. Immunoblotting was performed with either anti-LRP5 or anti-LRP6. (C) Effects of stable expression of an shRNA against LRP6 in 293T cells. Cultures were infected with a lentiviral vector containing the target sequence for LRP6 or a control vector in the presence of Polybrene (2 μg/ml) and marker selected with puromycin (2 μg/ml). Cell lysates were subjected to SDS-PAGE and immunoblotting with the anti-LRP6 MAb or with anti-tubulin as a loading control. (D) Comparison of endogenous and exogenous LRP6 expression levels and signaling activities. 293T cells were transfected with pCMV empty vector or pCMV-LRP6 plasmid (1 μg) in 100-mm plates. Total cell lysates (100 μg for the control and 10 μg for the LRP6-expressing cells) were subjected to SDS-PAGE and immunoblotting with anti-LRP6 (left). Analysis of uncomplexed β-catenin in the absence or presence of purified Wnt3a was performed by the GST–E-cadherin binding assay, utilizing 1 mg of lysates, as previously described (1) (middle and right).

vealed that both receptors were readily detectable and exhibited comparable levels of expression. As shown in Fig. 1A and B, one of the anti-LRP6 MAbs generated, clone 1C10, demonstrated high sensitivity in both Western blotting and immunoprecipitation assays and was specific to LRP6, as indicated by its lack of cross-reactivity with LRP5 under similar conditions. When the membranes were exposed for longer times, two major immunologic species, of approximately 200 to 220 kDa, were detected in untransfected 293T cells (data not shown).

To assess whether the signal observed was indeed endogenous LRP6, a short hairpin RNA (shRNA) lentiviral vector specific for LRP6 and containing a puromycin-selectable marker was generated for infection of 293T cells. The results showed that expression of the shRNA against LRP6 decreased the intensity of the two bands observed, confirming the specificity and high sensitivity of the generated MAb (Fig. 1C). Comparison of LRP6 levels normally present in 293T cells with those resulting from transient transfection of the receptor cDNA showed that endogenous LRP6 expression was 50- to 100-fold lower than that observed under conditions of overexpression (Fig. 1D). The results suggest that the receptor's normal function is exerted at expression levels considerably lower than those resulting from DNA transfection. In fact, analysis of uncomplexed β-catenin levels in these cells revealed that overexpressed LRP6 causes constitutive activation of the pathway in the absence of Wnt and enhanced sensitivity to a low concentration of the ligand. Thus, these findings strongly support the need for analysis of LRP6 function at physiological levels.

LRP6 is posttranslationally modified and is present at the cell surface in a dimeric form. Analysis of endogenous LRP6 in a series of normal and tumor cell lines revealed that the receptor is detectable as two distinct species similar to those observed in 293T cells (Fig. 2A). To analyze endogenous LRP6 posttranslational modifications, we exposed 293T cells to tunicamycin, a known inhibitor of N-glycosylation (40). Following exposure to increasing concentrations of tunicamycin, both LRP6 forms were progressively reduced to a single low-molecular-weight band. Similar results were obtained with COS-7 cells (Fig. 2B). To further assess LRP6 glycosylation, we subjected lysates from 293T cells to treatment with an N-glycosidase, PNGase F, which cleaves oligosaccharides from N-linked glycoproteins. The results indicated that following treatment with this enzyme, LRP6 mobility was altered, confirming receptor glycosylation (Fig. 2C). Cell surface biotinylation of NIH 3T3 cells followed by immunoprecipitation with streptavidin beads indicated that the higher-molecular-weight LRP6 species was predominant at the cell membrane and thus represents the signaling form of the receptor (Fig. 2D). To determine whether LRP6 modification by glycosylation is necessary for its localization at the cell membrane, we performed cell surface biotinylation analysis following treatment with increasing concentrations of tunicamycin. The progressive reduction of LRP6 to lower-molecular-weight forms in the total lysates resulted in a corresponding decrease in the receptor levels at the cell membrane, establishing that glycosylation is necessary for the cell surface localization of this receptor (Fig. 2E).

We have previously shown that LRP6 overexpressed in 293T cells forms non-disulfide-linked dimers (20). In order to analyze the molecular structure of the endogenous receptor, we performed chemical cross-linking using either a thiol-cleavable (DTSSP) or noncleavable (BS3) membrane-impermeative cross-linker. SDS-PAGE under nonreducing conditions of lysates from cells treated with BS3 or DTSSP revealed a dramatic decrease in the level of the cell surface-localized LRP6 form (Fig. 2F, left panel). These effects were reversed in the

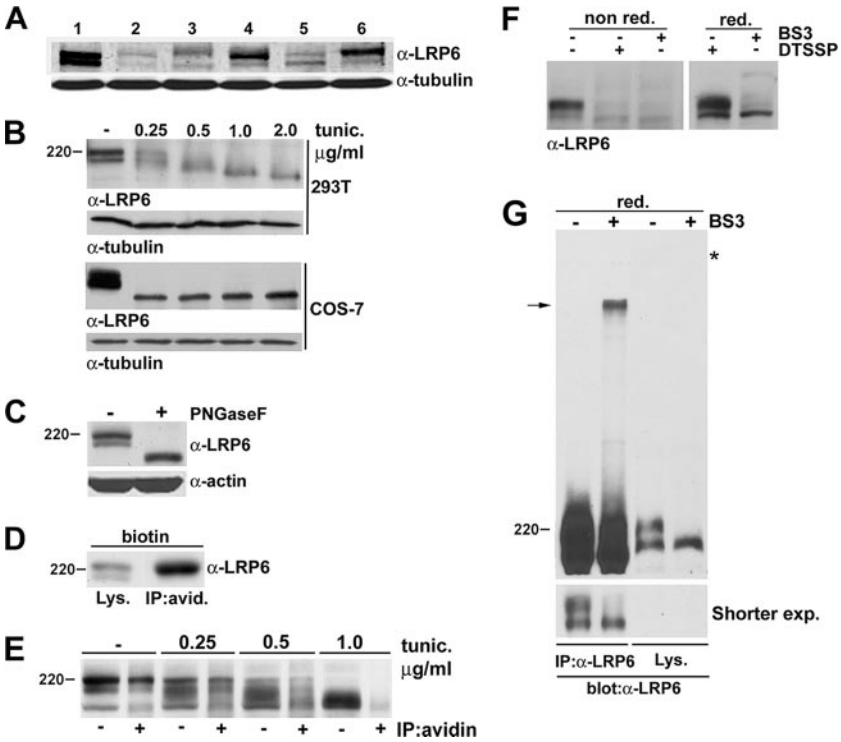

FIG. 2. Endogenous LRP6 is posttranslationally modified and is present at the cell surface in a multimolecular form. (A) Analysis of endogenous LRP6 protein in normal and tumor cell lines. Total cell lysates (100 μg) from NIH 3T3 (lane 1), AB589 (lane 2), MDAMB157 (lane 3), DU145 (lane 4), HCT116 (lane 5), and PA-1 (lane 6) cells were analyzed by immunoblotting with the anti-LRP6 MAb or the anti-tubulin antiserum as a loading control. (B) Effects of tunicamycin treatment on endogenous LRP6. 293T or COS7 cells were treated overnight with either dimethyl sulfoxide (DMSO) or the indicated amounts of tunicamycin (Sigma), and cell lysates were analyzed by immunoblotting with the LRP6 MAb. The same membranes were blotted with anti-tubulin as a loading control. (C) Effects of *N*-glycosidase treatment on LRP6 mobility. Cell lysates (70 μg) from 293T cells were denatured, treated for 2 h with PNGase F at 37°C, and analyzed by SDS-PAGE and immunoblotting with the anti-LRP6 antibody. (D) Cell surface biotinylation of NIH 3T3 cells. Cells were treated for 30 min with sulfo-NHS-LC-biotin (Pierce), and lysates were analyzed with the anti-LRP6 MAb directly or after immunoprecipitation with streptavidin beads. (E) Effects of tunicamycin treatment on the cell surface localization of LRP6. 293T cells were exposed to either a DMSO control or tunicamycin (0.25 to 1.0 μg/ml) overnight and then subjected to cell surface biotinylation. Lysates were analyzed with the anti-LRP6 MAb directly or after immunoprecipitation with streptavidin beads. (F and G) Analysis of LRP6 following treatment with cleavable and uncleavable cross-linkers. (F) 293T cells were incubated with BS3 or DTSSP in PBS for 20 min. Cell lysates were subjected to SDS-PAGE in the absence (left) or presence (right) of β-mercaptoethanol and subjected to immunoblotting with anti-LRP6. (G) Lysates of 293T cells treated with BS3 as described for panel F were analyzed for LRP6 levels directly or after immunoprecipitation with anti-LRP6. The bottom panel represents a shorter exposure. The asterisk indicates the beginning of the gel.

case of DTSSP-treated cell lysates when analysis was performed in the presence of the reducing agent β-mercaptoethanol (Fig. 2F, right panel). Although the signal corresponding to cell surface LRP6 was reduced to almost undetectable levels, no additional higher-molecular-weight bands were detectable by direct analysis of the lysates. Thus, in order to enrich for LRP6 complexes following BS3 treatment, cell lysates were subjected to immunoprecipitation with anti-LRP6 antibody prior to immunoblotting with the same antiserum. Analysis under these conditions revealed the presence of a slowly migrating species whose size is consistent with an LRP6 dimer (Fig. 2G). These results suggest that endogenous LRP6 exists at the cell membrane in a dimeric form.

Analysis of endogenous LRP6 phosphorylation under conditions of acute or chronic Wnt stimulation. There is evidence that upon Wnt stimulation, LRP6 is activated by phosphorylation at a series of sites present in its cytoplasmic domain (11, 34, 39). Analysis of endogenous LRP6 following treatment with purified Wnt3a in NIH 3T3 cells showed a decrease in the higher-molecular-weight species localized at the cell surface and the appearance of a slowly migrating form (Fig. 3A). Stimulation with purified Wnt5a under similar conditions had no effect, consistent with the reported inability of this ligand to induce canonical signaling in these cells (19) (Fig. 3A). Treatment of the Wnt3a-stimulated cell lysates with λ-phosphatase reverted the observed shift, confirming membrane-bound LRP6 phosphorylation (Fig. 3B). Moreover, preincubation of the cells with the soluble antagonist DKK1 completely blocked Wnt-induced LRP6 phosphorylation (Fig. 3C).

The ability to analyze endogenous LRP6 provided the opportunity to investigate the kinetics of its phosphorylation following Wnt stimulation. The results showed that receptor phosphorylation is detectable within 15 min of Wnt addition and is maintained for up to 6 h (Fig. 3D, top panel). The kinetics of uncomplexed β-catenin accumulation was also analyzed under similar conditions (Fig. 3D, bottom panel). A time course analysis of LRP6 phosphorylation levels following Wnt stimulation was also performed, utilizing the anti-phospho-LRP6 Ser1490 antibody, and the results were consistent with those obtained with the anti-LRP6 antiserum (Fig. 3E)

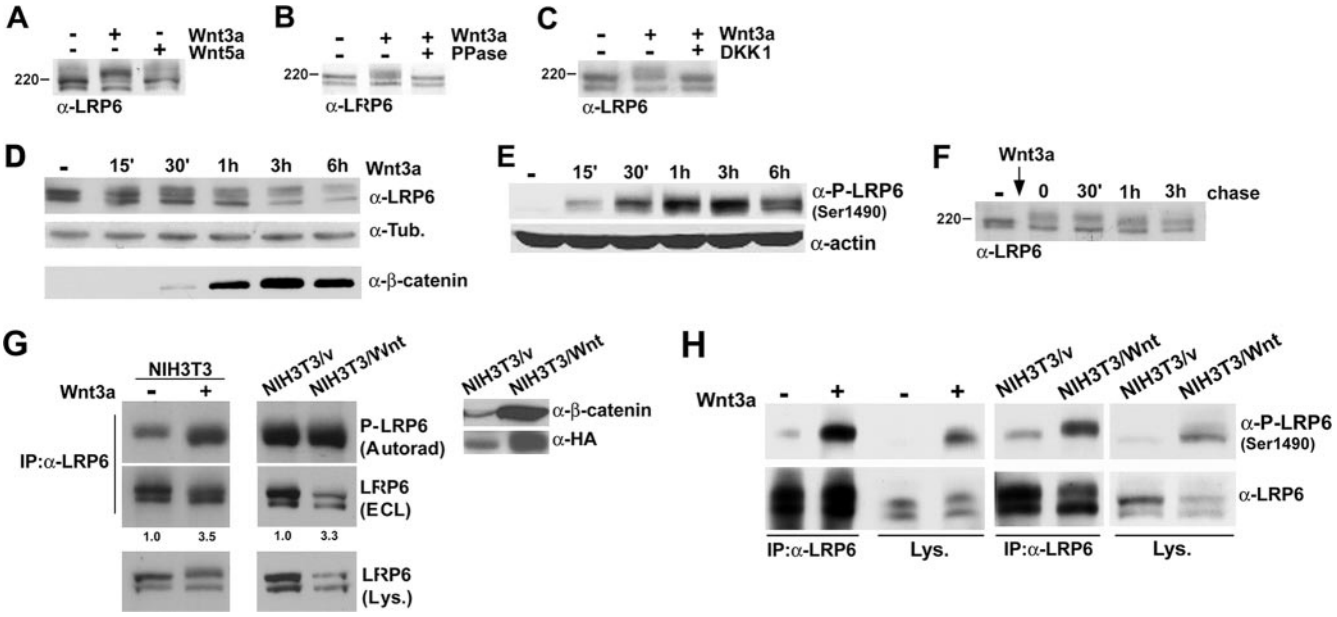

FIG. 3. Analysis of endogenous LRP6 phosphorylation under conditions of acute or chronic Wnt stimulation. (A) Wnt3a, but not Wnt5a, induces endogenous LRP6 mobility shift. Purified recombinant Wnt3a or Wnt5a (R&D Systems) at 100 ng/ml was added to NIH 3T3 cells for 1 h, and cell lysates were analyzed by SDS-PAGE followed by immunoblotting with the anti-LRP6 antibody. (B) Effects of phosphatase treatment on Wnt3a-induced LRP6 mobility shift. Following stimulation with Wnt3a as described for panel A, 293T cells were divided into two aliquots and lysed in either the presence or absence of phosphatase inhibitors. The latter was then subjected to λ-phosphatase treatment, and both lysates were analyzed by SDS-PAGE and immunoblotted with anti-LRP6 as described above. (C) Effects of DKK treatment on Wnt3a-induced LRP6 phosphorylation. 293T cells were incubated for 3 h with either control or DKK1-conditioned medium and then stimulated with Wnt3a as described for panel A. Lysates were analyzed with the anti-LRP6 MAb as described above. (D) Time course of LRP6 phosphorylation following Wnt stimulation. 293T cells were stimulated with purified Wnt3a for the indicated amounts of time, and cell lysates were analyzed by SDS-PAGE followed by immunoblotting with either the anti-LRP6 or anti-tubulin antibody (top and middle). Levels of uncomplexed β-catenin were measured by the GST–E-cadherin binding assay, as previously described (1), utilizing 500 μg of lysates (bottom). (E) Time course analysis of LRP6 phosphorylation in response to Wnt3a, utilizing a phospho-LRP6 antibody. 293T cells were treated with Wnt3a for the indicated amounts of time, and cell lysates (100 μg) were analyzed by SDS-PAGE followed by immunoblotting with the phospho-LRP6 (Ser1490) antibody or anti-actin as a loading control. (F) Analysis of LRP6 phosphorylation following removal of Wnt3a. After treatment of 293T cells with purified Wnt3a for 1 h, cells were washed and incubated with fresh growth medium. Cell lysates were collected at the indicated times following Wnt removal and analyzed as described for panel A. (G) Metabolic labeling of LRP6 in NIH 3T3 cells. Parental cells exposed to soluble recombinant Wnt3a for 2 h (left), NIH 3T3/vector cells, or NIH 3T3/Wnt3a-HA cells (right panels) were incubated with $^{32}PO_4$ as described in Materials and Methods and then immunoprecipitated with the LRP6 MAb. Following SDS-PAGE, samples were transferred and analyzed by autoradiography (top) or by immunoblotting with anti-LRP6 (middle). Cell lysates were also analyzed by Western blotting with anti-LRP6 (bottom). Uncomplexed β-catenin (700 μg) and Wnt3a (100 μg) levels were also measured in the same cell lysates, utilizing the anti-β-catenin and anti-HA antibodies, respectively (right). (H) Analysis of LRP6 phosphorylation by utilizing a phospho-LRP6 antibody. NIH 3T3 parental cells treated with recombinant Wnt3a, NIH 3T3/vector cells, or NIH 3T3/Wnt3a-HA cells were subjected to immunoprecipitation with the anti-LRP6 antibody and analyzed with either anti-LRP6 or anti-phospho-LRP6 (Ser1490). Total cell lysates were also analyzed directly with the same antibodies.

and with recent findings (35a). These findings raised the question of whether this phosphorylation, observed after several hours, was due to continuous ligand stimulation or maintained independent of the presence of Wnt3a. In order to distinguish between these two possibilities, cells were exposed to recombinant Wnt3a for 1 h and LRP6 was analyzed at several time points after removal of Wnt from the culture medium. As shown in Fig. 3F, LRP6 phosphorylation was unaffected 30 min following ligand withdrawal, attenuated at 1 h, and further reduced to almost undetectable levels at 3 h, suggesting that receptor activation is sustained but depends on the continuous presence of Wnt.

In order to more directly investigate endogenous LRP6 phosphorylation, we performed metabolic labeling of NIH 3T3 cells with [^{32}P]orthophosphate followed by immunoprecipitation analysis with the anti-LRP6 antibody. As indicated in Fig. 3G (top left panel), a signal corresponding to phospho-LRP6 was detectable in the untreated cells, suggesting that the receptor can be phosphorylated in a Wnt-independent manner. The addition of purified Wnt3a increased the signal for phospho-LRP6 3.5-fold, as determined by densitometry after normalization to total receptor levels detected by ECL analysis (Fig. 3G, top left panel). We next analyzed LRP6 phosphorylation under conditions of chronic ligand stimulation. For this purpose, we utilized NIH 3T3 cells in which constitutive autocrine Wnt signaling was established by retroviral infection with a Wnt3a-HA vector (Fig. 3G, right panel). Metabolic labeling of NIH 3T3 cells stably expressing Wnt3a resulted in an increase in LRP6 phosphorylation similar to that observed under conditions of acute ligand stimulation (Fig. 3G, middle panels). To further analyze LRP6 phosphorylation under acute or chronic conditions, NIH 3T3 cells either treated with recombinant Wnt3a or stably expressing this ligand were analyzed with the anti-phospho-LRP6 Ser1490 antibody directly or following immunoprecipitation with the anti-LRP6 antiserum (Fig. 3H). The results observed with this anti-phospho-LRP6

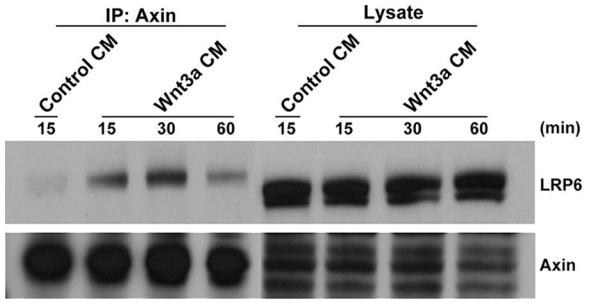

FIG. 4. Wnt-induced interaction of endogenous LRP6 and axin. 293T cells were treated with either control or Wnt3a-conditioned medium for the indicated amounts of time. Cell lysates were analyzed with an anti-axin antibody (Zymed) or the anti-LRP6 MAb either directly (100 μg) or following immunoprecipitation (1 mg) with anti-axin.

antibody were consistent with those obtained following in vivo metabolic labeling. All of these findings establish that chronic Wnt stimulation by either prolonged treatment with soluble ligand or autocrine signaling results in sustained receptor phosphorylation.

Wnt induces a rapid interaction between endogenous LRP6 and axin. Biochemical studies support a model by which Wnt-induced phosphorylation of LRP6 results in recruitment of axin to the cell membrane. Evidence for LRP6-axin interaction has been provided by studies involving their cotransfection in model cells (20, 22). Thus, in order to analyze the interaction between endogenous axin and LRP6 as well as to elucidate its kinetics in response to Wnt stimulation, 293T cells were exposed to Wnt3a-conditioned medium for increasing amounts of time. Immunoprecipitates obtained with the anti-axin antibody were analyzed with the same antiserum or the anti-LRP6 MAb. As shown in Fig. 4, while little or no interaction was observed in cells treated with control conditioned medium, LRP6 was detectable in complex with axin following Wnt stimulation. The results show that the interaction was detectable by 15 min, maximal at 30 min, and maintained for up to 1 h, providing evidence for recruitment of axin by LRP6 under physiological conditions.

Wnt induces LRP6 endocytosis and recycling to the cell surface. The lack of sensitive antibodies has so far hampered the analysis of endogenous LRP6 trafficking between the cell surface and the endosomal compartment in response to Wnt stimulation. Thus, we performed cell surface biotinylation of NIH 3T3 cells treated with purified Wnt3a for increasing amounts of time. Figure 5A shows that cell surface LRP6 levels decreased as early as 10 min following Wnt addition and were progressively reduced at 30 min and 1 h. Notably, following Wnt3a treatment for 3 h, cell surface LRP6 was restored to levels comparable to those observed in unstimulated cells (Fig. 5A, top panel). In an independent experiment, both cell surface and total LRP6 levels were compared for the same lysates, and the latter was found to be minimally or not affected by Wnt treatment for 1 or 3 h (Fig. 5A, bottom panel). These findings suggest that following Wnt stimulation, endogenous LRP6 is internalized and recycled back to the cell surface. Similar results were obtained in the presence of the protein synthesis inhibitor cycloheximide, indicating that the increase in cell surface LRP6 levels observed 3 h following Wnt stimulation could not be due to newly synthesized receptor (data not shown). In order to confirm LRP6 internalization, we performed Wnt stimulation followed by cell surface biotinylation at 4°C, conditions under which endocytosis is blocked. As indicated in Fig. 5B, no detectable changes in cell membrane-localized LRP6 levels were induced by Wnt treatment under these conditions. Analogous results came from analysis of Wnt effects on LRP6 at 37°C or 4°C in 293T cells (Fig. 5C). To determine whether the receptor could be internalized again following its recycling to the cell surface, we treated NIH 3T3 cells with Wnt3a for 1 and 3 h and then added fresh Wnt3a for 1 h. As shown in Fig. 5D, following internalization (1 h) and recycling (3 h), the levels of cell surface LRP6 were decreased again after treatment with fresh ligand for 1 hour, indicating that after being recycled, the receptor can undergo another round of internalization.

Internalization of cell surface receptors is mediated by either the clathrin-dependent pathway or the lipid raft-caveolin one (18). To gain insights into the route of LRP6 endocytosis, we analyzed the effects of nystatin and monodansylcadaverin (MDC), known inhibitors of the caveolin- and clathrin-dependent pathways, respectively (6, 12). As indicated in Fig. 5E, pretreatment of cells with either of these inhibitors prior to Wnt addition resulted in reduced LRP6 internalization. In contrast, neither nystatin nor MDC had any detectable effect on cell surface receptor levels in the absence of Wnt. The reduction of LRP6 internalization following transfection with an siRNA against clathrin further supports the involvement of this pathway (Fig. 5F). Together, these findings strongly suggest that in response to Wnt, LRP6 is internalized by a mechanism involving the caveolin- and clathrin-mediated pathways and is recycled to the cell surface.

Wnt signaling negatively regulates LRP6 expression at the transcriptional level. Having analyzed the effects of acute Wnt stimulation on LRP6, we next sought to investigate the receptor under conditions of chronic Wnt signaling. Cell surface biotinylation analysis of NIH 3T3 cells stably infected with Wnt3a-HA or control virus (Fig. 3G, right panel) indicated that constitutive Wnt3a expression resulted in a dramatic reduction in the levels of LRP6 localized at the cell membrane (Fig. 6A). Notably, analysis of cell lysates revealed that total LRP6 levels in NIH 3T3/Wnt3a cells were reduced as well (Fig. 6A). A similar decrease in receptor levels was noted during our studies of the kinetics of LRP6 phosphorylation when stimulation with soluble Wnt3a was carried out for three or more hours (Fig. 3D). These findings suggested that while acute Wnt stimulation induced receptor internalization and recycling, prolonged treatment with soluble ligand or chronic stimulation resulting from autocrine signaling decreased LRP6 steady-state levels.

In order to determine the mechanism responsible for the observed Wnt-induced decrease in LRP6 levels, we investigated the possibility that Wnt3a stimulation may increase its receptor's degradation. Thus, we treated NIH 3T3 control cells or NIH 3T3 cells expressing Wnt3a with the proteasomal inhibitor MG132 for increasing amounts of time and analyzed LRP6 protein levels. The results indicated that the receptor levels were not affected by inhibition of the proteasomal degradation pathway (Fig. 6B). As an internal control, the levels of

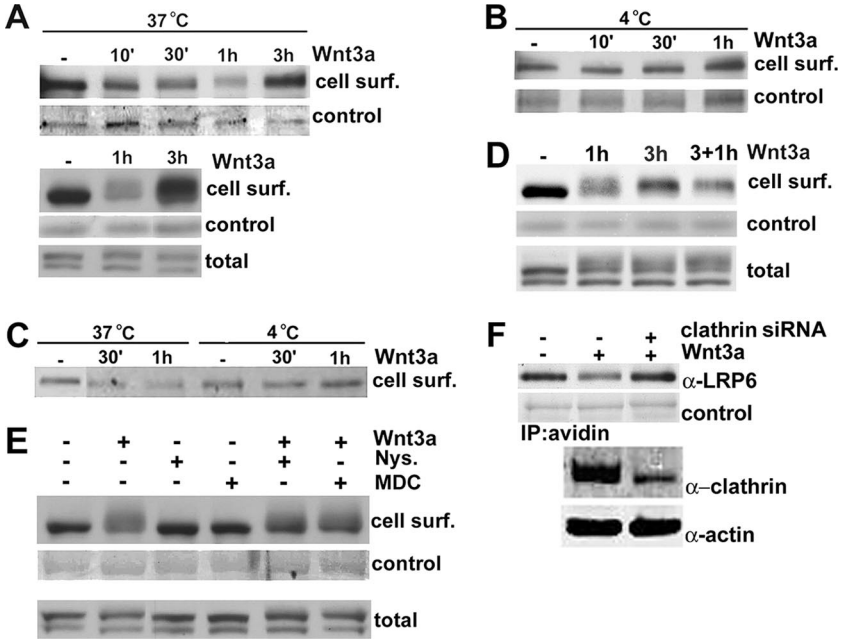

FIG. 5. Effects of acute Wnt stimulation on LRP6 cell surface localization. (A) Analysis of LRP6 cell surface localization following Wnt stimulation at 37°C. NIH 3T3 cells were incubated with purified Wnt3a (100 ng/ml) at 37°C for the indicated amounts of time and then subjected to biotinylation as described in the legend to Fig. 2D. Lysates (700 μg) were immunoprecipitated with streptavidin beads and analyzed by SDS-PAGE followed by immunoblotting with anti-LRP6 MAb. As a control for biotinylation efficiency, the membranes were immunoblotted with an anti-N-cadherin antibody (top) or stained with Coomassie blue (bottom). One hundred micrograms of cell lysates were also analyzed with anti-LRP6 for total receptor levels. (B) Analysis of cell surface LRP6 following Wnt stimulation at 4°C. NIH 3T3 cells were incubated with purified Wnt3a at 4°C and then analyzed as described for panel A. (C) Analysis of cell surface LRP6 levels in 293T cells following Wnt stimulation. Cultures were incubated with Wnt3a for the indicated amounts of time at either 37°C or 4°C and then analyzed as described for panel A. (D) Analysis of LRP6 internalization following its recycling to the cell surface. NIH 3T3 cells were treated with recombinant Wnt3a for 1, 3, or 3+1 h (cells were treated with Wnt3a for 3 h and then fresh Wnt3a was added for 1 h) and then subjected to cell surface biotinylation as described above. (E) Effects of inhibition of caveolin- or clathrin-dependent endocytosis on LRP6 internalization. Cells were pretreated with either a carrier control, nystatin (10 μg/ml), or MDC (30 μM) for 20 min and then treated with purified Wnt3a for 1 h in the presence of the inhibitor. Cells were subjected to biotinylation as described above, and cell surface (top) and total LRP6 (bottom) levels were detected with anti-LRP6. As a control for biotinylation efficiency, the membrane was stained with Coomassie blue (middle). (F) siRNA-mediated down-regulation of clathrin reduces Wnt3a-induced LRP6 internalization. HeLa cells were transfected with siRNA oligonucleotides (10 nM) directed against the clathrin heavy chain, using siPORT NeoFX transfection agent. After 48 h, cells were stimulated with purified Wnt3a (200 ng/ml) at 37°C for 1 h and then subjected to biotinylation as described in the legend to Fig. 2D. Lysates (1.0 mg) were immunoprecipitated with streptavidin beads, followed by SDS-PAGE and immunoblotting with anti-LRP6 MAb. As a control for biotinylation efficiency, the membranes were stained with Coomassie blue. Total cell lysates (40 μg) were also analyzed by immunoblotting to assess clathrin-heavy-chain knockdown by siRNA.

p53, a protein known to be degraded through proteasomes, were found to be increased in the same lysates. To analyze the effects of inhibition of the lysosome-mediated degradation pathway, NIH 3T3/vec and NIH 3T3/Wnt3a cells were treated for 2 hours with the lysosomal inhibitor chloroquine. As shown in Fig. 6C, LRP6 protein levels were unaffected following inhibition of this pathway. As a control, the PDGFR levels following stimulation with PDGF-BB were increased by chloroquine treatment in the same cells. Having excluded that Wnt-induced LRP6 down-regulation was due to increased receptor degradation, we investigated the possibility that Wnt may regulate LRP6 at the RNA level. For this purpose, we analyzed LRP6 mRNA expression levels by Northern blotting of NIH 3T3/Wnt3a or vector control cells. As shown in Fig. 6D, LRP6 transcript levels in NIH 3T3 cells were found to be reduced dramatically in response to Wnt expression. Similar results were obtained by quantitative real-time PCR analysis of the same cellular RNAs, establishing Wnt inhibition of its receptor's expression at the mRNA level (Fig. 6E). To gain insight into the kinetics of these inhibitory effects, we subjected parental NIH 3T3 cells to treatment with Wnt3a or control conditioned medium for increasing amounts of time and analyzed receptor protein and mRNA expression levels. Western blot analysis revealed that LRP6 protein levels were slightly reduced 3 h and further decreased 6 h following ligand addition (Fig. 6F). A consistent reduction was detected in the receptor transcript level by quantitative real-time PCR analysis of cellular RNAs extracted under the same conditions (Fig. 6G). In order to determine whether the effects on LRP6 RNA levels were due to transcriptional or posttranscriptional mechanisms, we analyzed the stability of the LRP6 transcript in the absence or presence of Wnt3a expression. NIH 3T3 vector or Wnt3a-expressing cells were treated with the transcription inhibitor actinomycin D for increasing amounts of time and analyzed by Northern blotting. The results showed that although the levels of LRP6 transcript in the Wnt3a-expressing cells were lower than those observed in the control cells, the rates of its degradation were comparable, excluding a role for posttranscriptional regulatory mechanisms (Fig. 6H). Together, all of these findings provide evidence for a

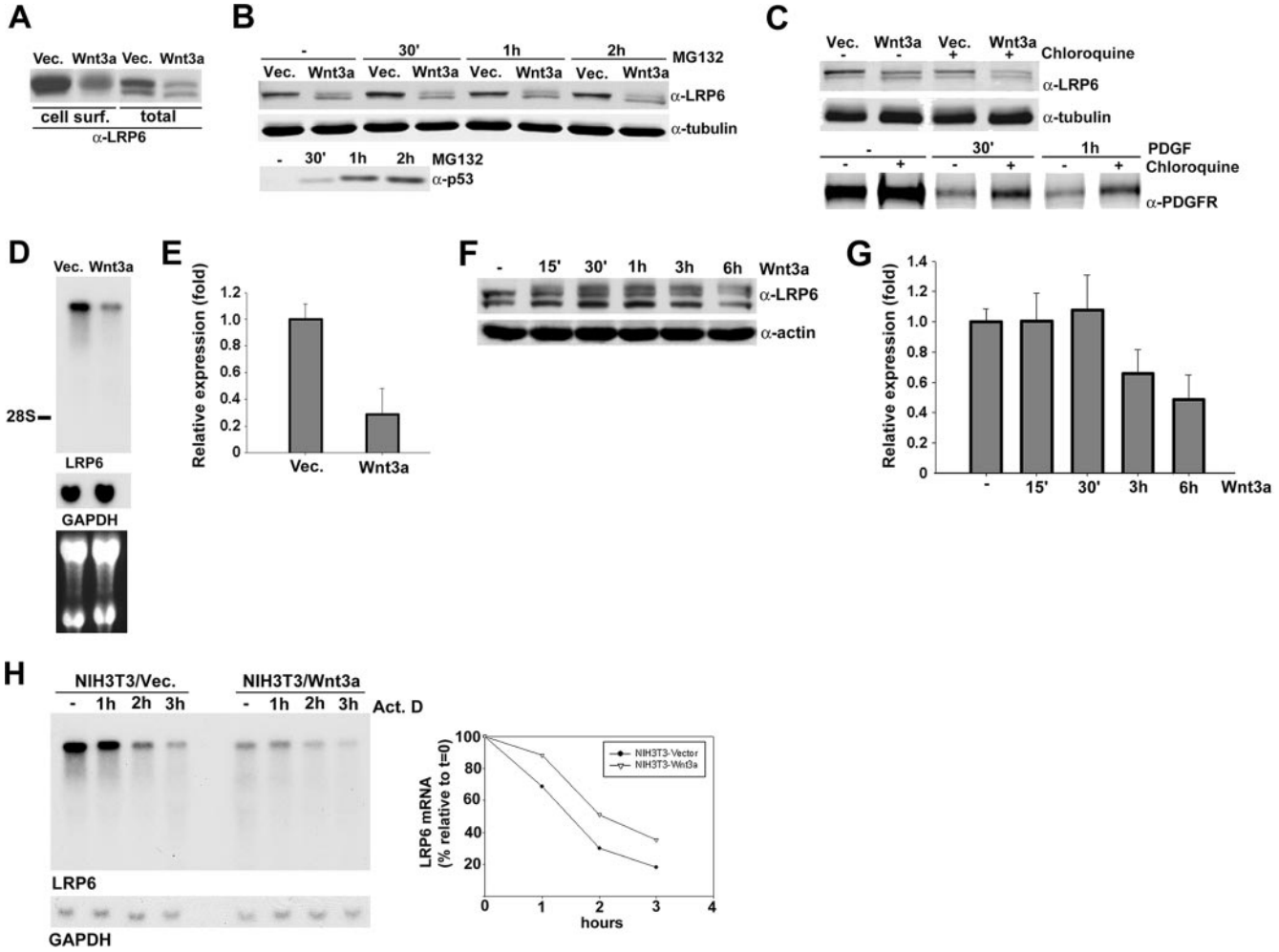

FIG. 6. Wnt signaling negatively regulates LRP6 expression at the transcriptional level. (A) Effects of autocrine Wnt signaling on cell surface and total LRP6 levels. NIH 3T3 cells stably expressing either Wnt3a-HA or the empty vector were subjected to biotin treatment, and 700 μg of total cell lysate was analyzed by immunoprecipitation with streptavidin beads as described in the legend to Fig. 5. Lysates (100 μg) were also analyzed directly for total LRP6 levels. (B) Effects of the proteasomal inhibitor MG132 on LRP6 protein levels. NIH 3T3/vector and NIH 3T3/Wnt3a cells were treated with MG132 (50 μM) or DMSO control for the indicated amounts of time. Lysates were analyzed by Western blotting with the anti-LRP6 (top) or anti-tubulin (middle) antibody. The same lysates were also analyzed with an antibody to p53 (bottom). (C) Effects of lysosomal inhibition on LRP6 protein levels. NIH 3T3/vector and NIH 3T3/Wnt3a cells were treated with the lysosomal inhibitor chloroquine or with PBS for 2 h, and lysates were analyzed with the anti-LRP6 (top) or anti-tubulin (middle) antibody. NIH 3T3 vector cells were treated with PDGF-BB for the indicated amounts of time and analyzed with the PDGFR antibody (bottom). (D) Northern blot analysis of LRP6 transcripts in NIH 3T3 cells stably expressing Wnt3a. Total RNAs (20 μg) were electrophoresed in a formaldehyde-agarose gel and transferred to a nylon membrane. Hybridization was performed with a 430-bp PCR-amplified, ^{32}P-labeled mouse LRP6 or glyceraldehyde-3-phosphate dehydrogenase (GAPDH) probe. The position of the 28S rRNA is indicated. The lower panel displays an image of the ethidium bromide-stained gel. (E) Real-time PCR analysis of LRP6 mRNA expression in NIH 3T3 cells stably expressing Wnt3a. Real-time PCR was conducted as described in Materials and Methods, utilizing primers specific for mouse LRP6, and the results were normalized to TATA box binding protein expression levels. The values represent one of two independently performed experiments done in triplicate. (F) Kinetics of Wnt3a-induced down-regulation of LRP6 protein levels. NIH 3T3 cells were treated with either control or Wnt3a-conditioned medium for the indicated times. Cell lysates (100 μg) were analyzed by Western blotting with anti-LRP6 MAb or anti-β-actin as a loading control. (G) Kinetics of Wnt3a-induced down-regulation of LRP6 transcript expression. Total RNAs were extracted from cells treated as described for panel F, and real-time PCR was conducted with primers specific to mouse LRP6, with the results normalized to TATA box binding protein levels. The values are from a representative experiment performed in triplicate. (H) Analysis of LRP6 transcript stability. NIH 3T3/vector and NIH 3T3/Wnt3a cells were treated with actinomycin D (7.5 μg/ml) for the indicated amounts of time. Northern blot analysis was performed as described for panel D. The graph represents an analysis by densitometry following normalization with GAPDH.

novel feedback mechanism by which Wnt negatively regulates LRP6 transcription.

Wnt-induced inhibition of LRP6 transcription is mediated by β-catenin. Wnt signaling activation inhibits the phosphorylation and subsequent degradation of β-catenin, which translocates to the nucleus and, through interaction with the TCF/LEF transcription factors, activates gene expression (9). To determine whether the Wnt effects on LRP6 were mediated by the β-catenin/TCF complex, we stably infected NIH 3T3/Wnt3a cells with a lentivirus containing a dominant-negative

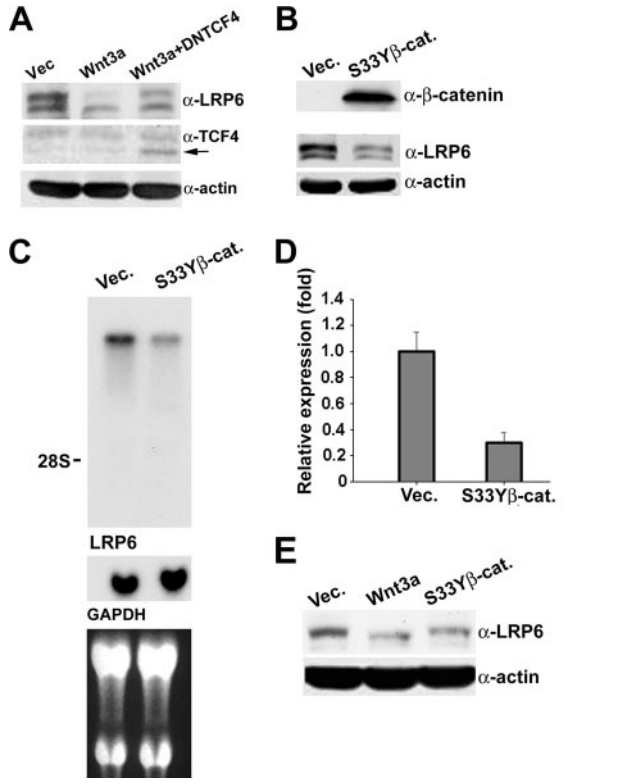

FIG. 7. Wnt-induced inhibition of LRP6 RNA expression is mediated by β-catenin. (A) Effects of DNTCF4 on Wnt-induced downregulation of LRP6. NIH 3T3 cells expressing Wnt3a were infected with a lentiviral construct expressing DNTCF4 and selected with puromycin (2 μg/ml) for 2 weeks. Cell lysates (50 μg) were analyzed with the anti-LRP6 (top), anti-TCF4 (middle), or anti-actin (bottom) antibody. (B) Analysis of total LRP6 protein level in NIH 3T3 cells stably expressing mutant β-catenin. NIH 3T3 cells were infected with either mutant β-catenin S33Y or control retrovirus. After marker selection for 2 weeks, cell lysates (100 μg) were subjected to the GST–E-cadherin binding assay to determine uncomplexed β-catenin levels (top). The same lysates (50 μg) were analyzed with anti-LRP6 MAb (middle) or with anti-β-actin as a loading control (bottom). (C) Northern blot analysis of LRP6 transcripts in NIH 3T3 cells overexpressing mutant β-catenin. Total RNAs (20 μg) electrophoresed in a formaldehyde-agarose gel were transferred to a nylon membrane and probed with a 430-bp PCR-amplified, ^{32}P-labeled mouse LRP6 or GAPDH probe. The position of the 28S rRNA is indicated. The lower panel displays an image of the ethidium bromide-stained gel. (D) Real-time PCR analysis of LRP6 transcript expression in NIH 3T3 cells stably expressing mutant β-catenin. The same RNAs utilized for panel C were subjected to real-time PCR analysis as described in the legend to Fig. 6E. The values were derived from a representative experiment performed in triplicate. (E) Analysis of total LRP6 protein levels in AB589 human breast epithelial cells stably expressing Wnt3a or mutant β-catenin. Cells were infected with either Wnt3a-HA, β-catenin S33Y, or control retrovirus. Following 2 weeks of marker selection, cell lysates (100 μg) were analyzed by Western blotting with anti-LRP6 MAb (top) or with anti-β-actin as a loading control (bottom).

form of TCF4 which lacks the β-catenin binding domain (DNTCF4). Analysis of LRP6 protein levels revealed that even low levels of DNTCF4 resulted in an increase in LRP6 protein expression, implicating the TCF/LEF transcription factors as mediators of the observed Wnt effects (Fig. 7A). We next stably infected NIH 3T3 cells with a retroviral construct encoding a mutant form of β-catenin, β-catenin S33Y, which is resistant to phosphorylation and degradation (25). Analysis of uncomplexed β-catenin levels indicated constitutive pathway activation induced by expression of this mutant form of β-catenin in NIH 3T3 cells. Western blot analysis of LRP6 revealed that, similar to the case observed under conditions of chronic Wnt stimulation, expression of β-catenin S33Y dramatically decreased the steady-state levels of the receptor (Fig. 7B). Northern blot and real-time PCR analyses indicated that the decrease in LRP6 levels was due to reduced expression at the RNA level (Fig. 7C and D). These results strongly implicate the β-catenin/TCF heterodimer as the mediator of the negative regulation of LRP6 by Wnt.

In order to generalize these findings, we infected the immortalized breast epithelial cell line AB589 with the Wnt3a and β-catenin S33Y retroviruses. Western blot analysis of LRP6 indicated that constitutive expression of Wnt3a or mutant β-catenin strongly reduced receptor steady-state levels in this cell line as well (Fig. 7E). These findings provide evidence for a new level of ligand-induced LRP6 regulation by which Wnt inhibits its receptor's RNA expression level through a β-catenin/TCF-mediated mechanism.

DISCUSSION

The evolutionarily conserved canonical Wnt pathway plays a critical role in embryonic development, and its deregulation is implicated in human bone diseases and tumorigenesis (7, 9, 36). Because of the difficulties in generating immunological reagents, our understanding of Wnt signaling through its receptors has relied on studies involving protein overexpression. In the present study, using a highly specific and sensitive MAb, we have shown that endogenous LRP6 is expressed at considerably lower (>50-fold) levels than those resulting from its overexpression. Indeed, exogenous LRP6 expression resulted in constitutive activation of the pathway in the absence of Wnt and dramatically enhanced ligand sensitivity, supporting the need for analysis of the receptor at physiological expression levels.

Characterization of endogenous LRP6 revealed that the receptor is posttranslationally modified by N-glycosylation and that this modification is necessary for its cell surface localization. Two previous studies reached different conclusions concerning LRP6 dimerization in the absence or presence of Wnt stimulation (10, 20). Our findings indicating the presence of LRP6 dimers in unstimulated 293T cells are in accordance with those of Liu et al., suggesting that the LRP6 dimeric complexes are inactive. Whether LRP6 forms homo- or heterodimeric complexes as well as higher-order oligomers remains to be determined. Analysis of the kinetics of receptor activation revealed that, unlike that of certain receptors that are rapidly and transiently phosphorylated following ligand binding (31), phosphorylation of endogenous LRP6 in response to Wnt is sustained and the receptor is not desensitized by chronic ligand stimulation. However, sustained phosphorylation of the receptor depends on Wnt, and ligand removal causes slow dephosphorylation of LRP6. Consistent with the current model that phosphorylated LRP6 recruits axin from the cytoplasm (22), we provide the first evidence for complex formation between endogenous LRP6 and axin under conditions of Wnt stimulation. Since axin recruitment is believed to occur in a cyclical

manner, sustained receptor phosphorylation may be necessary to ensure the continued shuttling of axin from the cytoplasm to the cell membrane.

Analysis of cell surface biotinylation revealed that Wnt stimulation induces progressive internalization of endogenous LRP6. A previous report indicated that Wnt induces exogenous LRP6 endocytosis through the caveolin-mediated pathway (38). In contrast, there is evidence suggesting that internalization of Wingless is mediated through clathrin (6). Our results showing that LRP6 internalization is decreased in the presence of inhibitors of either clathrin- or caveolin-mediated endocytosis may explain these discrepancies, providing evidence for the involvement of both pathways in the internalization of endogenous LRP6. Many cell surface receptors are either targeted for lysosomal degradation or recycled to the plasma membrane following ligand-induced internalization. Our observations indicate that following Wnt-induced endocytosis, LRP6 is recycled back to the cell surface within hours of the initial stimulus.

Finally, we have identified a novel feedback mechanism of receptor regulation by which Wnt down-regulates LRP6 and have provided evidence that the effects observed are not due to increased ligand-induced LRP6 degradation but, rather, occur at the RNA level. Our analysis of LRP6 transcript stability indicated that posttranscriptional mechanisms are not involved. Additionally, overexpression of a stable form of β-catenin or DNTCF4 provided evidence that the Wnt-induced transcriptional effects are mediated through the β-catenin/TCF complex. Whether LRP6 is a direct or indirect target of β-catenin/TCF remains to be determined. However, since the β-catenin/TCF heterodimer has been shown to act as a transcriptional activator rather than a repressor, we can speculate that the effects on LRP6 transcription are likely to be indirect. Notably, earlier studies of *Drosophila* embryos reported that after the onset of zygotic transcription, *arrow* RNA levels appeared to be reduced in cells expressing Wingless, although the mechanism responsible for these effects was not investigated (35).

Ligand-induced receptor "down-regulation" is a common mechanism for receptor modulation and is believed to be essential in ensuring attenuation of cellular signals. For some receptors, such as G-protein-coupled receptors, down-regulation is achieved by internalization and subsequent degradation (15), while for others, such as hormone receptors, ligand-induced down-regulation occurs at the transcriptional level (4, 29). Interestingly, the LDL receptor, which is structurally related to LRP6, undergoes repeated rounds of endocytosis followed by recycling and is also regulated by its ligands at the mRNA level (30).

The critical role of the canonical Wnt pathways in many developmental processes and the evidence that its improper activation leads to human disease (9, 36) predict the need for mechanisms that regulate Wnt signaling. The existence of several naturally occurring Wnt antagonists, such as FRP and DKK, which spatially and temporally modulate Wnt activity, supports this hypothesis (16). Our identification of Wnt-induced inhibition of LRP6 RNA expression uncovers a new mechanism by which this pathway is regulated. The possibility that the aberrant activation of Wnt signaling may in some cases involve the loss of this negative feedback mechanism has important implications concerning therapeutic strategies aimed at targeting the LRP6 receptor.

ACKNOWLEDGMENTS

The anti-LRP6 MAb was generated in collaboration with Thomas Moran (Hybridoma Center, Mount Sinai School of Medicine, NY).

This work was supported by a grant from the U.S. Department of Defense (DAMD17-03-1-0268), the Breast Cancer Research Foundation, and a grant from the NIH/NCI (1 R01 CA121119-01A1). Teresa Villanueva de la Torre is supported by Fundacion Alfonso Martin Escudero, Madrid, Spain.

REFERENCES

1. **Bafico, A., A. Gazit, S. S. Wu-Morgan, A. Yaniv, and S. A. Aaronson.** 1998. Characterization of Wnt-1 and Wnt-2 induced growth alterations and signaling pathways in NIH3T3 fibroblasts. Oncogene **16:**2819–2825.
2. **Bafico, A., G. Liu, L. Goldin, V. Harris, and S. A. Aaronson.** 2004. An autocrine mechanism for constitutive Wnt pathway activation in human cancer cells. Cancer Cell **6:**497–506.
3. **Bafico, A., G. Liu, A. Yaniv, A. Gazit, and S. A. Aaronson.** 2001. Novel mechanism of Wnt signalling inhibition mediated by Dickkopf-1 interaction with LRP6/Arrow. Nat. Cell Biol. **3:**683–686.
4. **Bellingham, D. L., M. Sar, and J. A. Cidlowski.** 1992. Ligand-dependent down-regulation of stably transfected human glucocorticoid receptors is associated with the loss of functional glucocorticoid responsiveness. Mol. Endocrinol. **6:**2090–2102.
5. **Bhanot, P., M. Brink, C. H. Samos, J. C. Hsieh, Y. Wang, J. P. Macke, D. Andrew, J. Nathans, and R. Nusse.** 1996. A new member of the frizzled family from Drosophila functions as a Wingless receptor. Nature **382:**225–230.
6. **Blitzer, J. T., and R. Nusse.** 2006. A critical role for endocytosis in Wnt signaling. BMC Cell Biol. **7:**28.
7. **Cadigan, K. M., and R. Nusse.** 1997. Wnt signaling: a common theme in animal development. Genes Dev. **11:**3286–3305.
8. **Chen, W., D. ten Berge, J. Brown, S. Ahn, L. A. Hu, W. E. Miller, M. G. Caron, L. S. Barak, R. Nusse, and R. J. Lefkowitz.** 2003. Dishevelled 2 recruits beta-arrestin 2 to mediate Wnt5A-stimulated endocytosis of Frizzled 4. Science **301:**1391–1394.
9. **Clevers, H.** 2006. Wnt/beta-catenin signaling in development and disease. Cell **127:**469–480.
10. **Cong, F., L. Schweizer, and H. Varmus.** 2004. Wnt signals across the plasma membrane to activate the beta-catenin pathway by forming oligomers containing its receptors, Frizzled and LRP. Development **131:**5103–5115.
11. **Davidson, G., W. Wu, J. Shen, J. Bilic, U. Fenger, P. Stannek, A. Glinka, and C. Niehrs.** 2005. Casein kinase 1 gamma couples Wnt receptor activation to cytoplasmic signal transduction. Nature **438:**867–872.
12. **Di Guglielmo, G. M., C. Le Roy, A. F. Goodfellow, and J. L. Wrana.** 2003. Distinct endocytic pathways regulate TGF-beta receptor signalling and turnover. Nat. Cell Biol. **5:**410–421.
13. **Gordon, M. D., and R. Nusse.** 2006. Wnt signaling: multiple pathways, multiple receptors, and multiple transcription factors. J. Biol. Chem. **281:**22429–22433.
14. **He, X., M. Semenov, K. Tamai, and X. Zeng.** 2004. LDL receptor-related proteins 5 and 6 in Wnt/beta-catenin signaling: arrows point the way. Development **131:**1663–1677.
15. **Katzmann, D. J., G. Odorizzi, and S. D. Emr.** 2002. Receptor downregulation and multivesicular-body sorting. Nat. Rev. Mol. Cell. Biol. **3:**893–905.
16. **Kawano, Y., and R. Kypta.** 2003. Secreted antagonists of the Wnt signalling pathway. J. Cell Sci. **116:**2627–2634.
17. **Kikuchi, A., H. Yamamoto, and S. Kishida.** 2007. Multiplicity of the interactions of Wnt proteins and their receptors. Cell. Signal. **19:**659–671.
18. **Le Roy, C., and J. L. Wrana.** 2005. Clathrin- and non-clathrin-mediated endocytic regulation of cell signalling. Nat. Rev. Mol. Cell. Biol. **6:**112–126.
19. **Liu, G., A. Bafico, and S. A. Aaronson.** 2005. The mechanism of endogenous receptor activation functionally distinguishes prototype canonical and noncanonical Wnts. Mol. Cell. Biol. **25:**3475–3482.
20. **Liu, G., A. Bafico, V. K. Harris, and S. A. Aaronson.** 2003. A novel mechanism for Wnt activation of canonical signaling through the LRP6 receptor. Mol. Cell. Biol. **23:**5825–5835.
21. **Mao, B., W. Wu, Y. Li, D. Hoppe, P. Stannek, A. Glinka, and C. Niehrs.** 2001. LDL-receptor-related protein 6 is a receptor for Dickkopf proteins. Nature **411:**321–325.
22. **Mao, J., J. Wang, B. Liu, W. Pan, G. H. Farr III, C. Flynn, H. Yuan, S. Takada, D. Kimelman, L. Li, and D. Wu.** 2001. Low-density lipoprotein receptor-related protein-5 binds to axin and regulates the canonical Wnt signaling pathway. Mol. Cell **7:**801–809.
23. **Mikels, A. J., and R. Nusse.** 2006. Wnts as ligands: processing, secretion and reception. Oncogene **25:**7461–7468.
24. **Moon, R. T., A. D. Kohn, G. V. De Ferrari, and A. Kaykas.** 2004. WNT and beta-catenin signalling: diseases and therapies. Nat. Rev. Genet. **5:**691–701.

25. **Morin, P. J., A. B. Sparks, V. Korinek, N. Barker, H. Clevers, B. Vogelstein, and K. W. Kinzler.** 1997. Activation of beta-catenin-Tcf signaling in colon cancer by mutations in beta-catenin or APC. Science **275:**1787–1790.
26. **Neel, N. F., E. Schutyser, J. Sai, G. H. Fan, and A. Richmond.** 2005. Chemokine receptor internalization and intracellular trafficking. Cytokine Growth Factor Rev. **16:**637–658.
27. **Pinson, K. I., J. Brennan, S. Monkley, B. J. Avery, and W. C. Skarnes.** 2000. An LDL-receptor-related protein mediates Wnt signalling in mice. Nature **407:**535–538.
28. **Polakis, P.** 2000. Wnt signaling and cancer. Genes Dev. **14:**1837–1851.
29. **Rosewicz, S., A. R. McDonald, B. A. Maddux, I. D. Goldfine, R. L. Miesfeld, and C. D. Logsdon.** 1988. Mechanism of glucocorticoid receptor down-regulation by glucocorticoids. J. Biol. Chem. **263:**2581–2584.
30. **Russell, D. W., T. Yamamoto, W. J. Schneider, C. J. Slaughter, M. S. Brown, and J. L. Goldstein.** 1983. cDNA cloning of the bovine low density lipoprotein receptor: feedback regulation of a receptor mRNA. Proc. Natl. Acad. Sci. USA **80:**7501–7505.
31. **Schlessinger, J.** 2000. Cell signaling by receptor tyrosine kinases. Cell **103:** 211–225.
32. **Semenov, M. V., K. Tamai, B. K. Brott, M. Kuhl, S. Sokol, and X. He.** 2001. Head inducer Dickkopf-1 is a ligand for Wnt coreceptor LRP6. Curr. Biol. **11:**951–961.
33. **Tamai, K., M. Semenov, Y. Kato, R. Spokony, C. Liu, Y. Katsuyama, F. Hess, J. P. Saint-Jeannet, and X. He.** 2000. LDL-receptor-related proteins in Wnt signal transduction. Nature **407:**530–535.
34. **Tamai, K., X. Zeng, C. Liu, X. Zhang, Y. Harada, Z. Chang, and X. He.** 2004. A mechanism for Wnt coreceptor activation. Mol. Cell **13:**149–156.
35. **Wehrli, M., S. T. Dougan, K. Caldwell, L. O'Keefe, S. Schwartz, D. Vaizel-Ohayon, E. Schejter, A. Tomlinson, and S. DiNardo.** 2000. *arrow* encodes an LDL-receptor-related protein essential for Wingless signalling. Nature **407:** 527–530.
35a. **Wei, Q., C. Yokota, M. V. Semenov, B. Doble, J. Woodgett, and X. He.** 2007. R-spondin1 is a high affinity ligand for LRP6 and induces LRP6 phosphorylation and beta-catenin signaling. J. Biol. Chem. **282:**15903–15911.
36. **Westendorf, J. J., R. A. Kahler, and T. M. Schroeder.** 2004. Wnt signaling in osteoblasts and bone diseases. Gene **341:**19–39.
37. **Wiley, H. S.** 2003. Trafficking of the ErbB receptors and its influence on signaling. Exp. Cell Res. **284:**78–88.
38. **Yamamoto, H., H. Komekado, and A. Kikuchi.** 2006. Caveolin is necessary for Wnt-3a-dependent internalization of LRP6 and accumulation of beta-catenin. Dev. Cell **11:**213–223.
39. **Zeng, X., K. Tamai, B. Doble, S. Li, H. Huang, R. Habas, H. Okamura, J. Woodgett, and X. He.** 2005. A dual-kinase mechanism for Wnt co-receptor phosphorylation and activation. Nature **438:**873–877.
40. **Zhou, Y. B., F. Liu, Z. D. Zhu, H. Zhu, X. Zhang, Z. Q. Wang, J. H. Liu, and Z. G. Han.** 2004. N-glycosylation is required for efficient secretion of a novel human secreted glycoprotein, hPAP21. FEBS Lett. **576:**401–407.